JOURNAL OF AGRICULTURAL AND FOOD CHEMISTRY

ARTICLE

pubs.acs.org/JAFC

Textural Properties and Their Correlation to Cell Structure in Porous Food Materials

Nesli Sozer,[†] Hulya Dogan,[§] and Jozef L. Kokini*[,†]

[†]Department of Food Science and Human Nutrition, University of Illinois at Urbana−Champaign, Urbana, Illinois 61801, United States

[§]Department of Grain Science and Industry, Kansas State University, Manhattan, Kansas 66506, United States

ABSTRACT: This paper focuses on understanding the role of structural parameters and starch crystallization on the toughness of cake samples. Accurate mechanical measurements were performed to obtain toughness values, and these were related to structural parameters obtained from image analyses. Three-dimensional skeletons of food samples were generated by using X-ray tomography technique. The structural parameters (cell diameter, cell wall thickness, thickness to radius ratio (t/R), fragmentation index) were obtained after processing of the images with CTan software. The basic hypothesis of the paper is to show that the structural parameter t/R is a determinant for predicting toughness, which is a critical indicator of freshness. Freshness in cakes and other baked products is a leading factor in consumer perception. For this purpose three different cake formulations were stored at 37 and 50 °C. Cycling from these temperatures to lower storage temperatures of 25 and 4 °C was done to accelerate the starch retrogradation rate. Experimental results indicated that there was a strong interrelationship between morphological structure and the mechanical properties with regression coefficients of 0.68 and 0.95. Starch retrogradation, which was followed by X-ray diffractometry, was found to be directly proportional to toughness values, where the percent relative crystallinity increased with storage temperature.

KEYWORDS: X-ray microtomography, X-ray diffractometer, cellular structure, texture, mechanical properties

INTRODUCTION

Consumer acceptance of solid food foams such as breads, cakes, and extruded snacks is strongly associated with the product texture. The mechanical properties of cellular foods and in particular their fracture behaviors are known to be related to both the mechanical properties of polymeric cell walls and the average size and size distribution of the air cells in solid food foams. The structure and state of the solid matrix control the deformation pathway of the food material, such as elastoplastic or brittle failure, which in turn has an effect on the force-deformation curves. The cellular structure of food materials, in both macro (porosity and relative density) and micro (cell wall thickness, cell diameter, and their distributions) scales, also influences mechanical properties. Sensorial attributes of food foams are dependent on cell size and its distribution, shape of cells, and cell wall thickness. Understanding the effect of structural parameters on food foam will allow food designers to evaluate the effect of processing conditions and ingredients on sensorial perception.[1,2]

The cellular structure of solid food foams is highly influenced by processing conditions (mixing, proofing, baking), ingredient composition, and their interactions. The heterogeneous morphology of cellular solid foods makes the quantification of structure/mechanical relationships complex. Basic solid mechanics theories have been applied by several researchers to define the fundamental mechanical behavior of various food products.[3,4] Several techniques have been used to study food microstructures and these include microscopy,[5,6] magnetic resonance imaging,[7,8] computer vision technique,[9,10] porosimetry,[11,12] and most recently X-ray computed tomography.[13−15]

The advent of powerful noninvasive techniques such as X-ray microtomography (XMT) has enabled better characterization of porous food structures compared to other techniques such as density measurement. The specimen is targeted with a polychromatic X-ray beam with high spatial coherence. The X-rays not absorbed by the specimen fall on specifically designed X-ray scintillators that produce visible light, which is then recorded by a charge-coupled device (CCD) camera. A tomographic scan is accomplished by rotating the specimen between a fixed X-ray source and detector, around the axis perpendicular to the X-ray beam, while collecting radiographs of the specimen at small angular increments in the range of 0−360°. The radiographs are reconstructed into a series of 2-D slices. The series of 2-D slices are then reconstructed into a 3-D image. The resulting XMT data can be visualized by 3-D rendering or 2-D slices derived from virtual model using dedicated software that allows reconstruction of cross sections at various depth increments and along any desired orientation of the plane of cut.

Up to now, most of the microtomography studies were made on bread crumb, for which scientists evaluated the effect of ingredients on bread crumb structure.[16,17] The authors were able to calculate the smallest dimension of the wall by morphological granulometry through the X-ray tomography images. Lassoud et al.[16] showed that the results obtained from 2-D images acquired by flat bed scanning technique were comparable to those from 3-D images obtained with a robust XMT technique. Dogan et al.[18] showed that cell wall structure, cell size, and its distribution

Special Issue: Food Texture Analysis in the 21st Century

Received: February 16, 2010
Revised: December 29, 2010
Accepted: January 10, 2011
Published: February 09, 2011

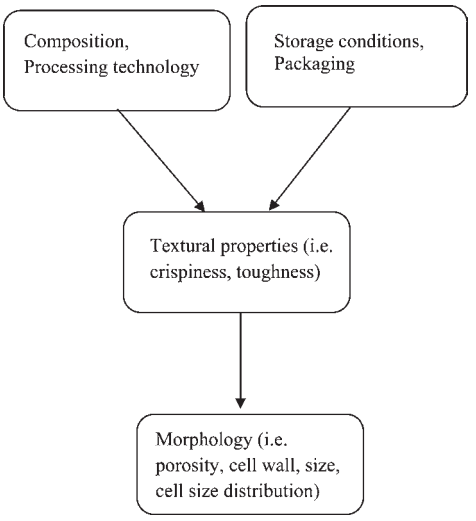

Figure 1. Factors affecting food material properties.

within the food matrix influence the mechanical properties of solid food foams as well as consumer acceptance.

Szczesniak[19] suggested that there are several senses involved in the texture perception of foods. For cakes, which are soft cellular solid foods, the fresh baked odor, crust color, and sweet flavor act together to affect the perception of freshness and softness, whereas for extruded snack foods the brittle-crisp texture is an indicator of freshness. Psychophysical models can be used to evaluate the effect of formulation and processing on the texture sensation of food materials.[1]

Figure 1 represents the factors that affect food material properties of cellular solid foods. In this figure we link how processing technology and storage conditions affect structural properties and morphology, which in turn affect mechanical and textural properties.

The microstructural features (average cell size, cell size distribution, cell wall thickness, and resulting porosity) control textural properties, along with the material properties and phase behavior of the cell wall (Figure 2). However, there is still a lack of scientific understanding on how foam structure in baked goods influences the other quality parameters. This study focused on evaluating the three-dimensional image analyses of X-ray microtomography data as a novel imaging technique to understand the effect of ingredients and storage conditions on microstructural characteristics and their relationships to textural parameters.

MATERIALS AND METHODS

Materials. Flour (Purasnow Cake Flour, General Mills, Minneapolis, MN, with 8.2% protein and 14% moisture content), sugar (Domino, American Sugar Refining, Inc.), dried egg powder (Rembrant Foods, Abbeville, AL), shortening (Solae, St. Louis, MO), cocoa powder (De Zaan, The Netherlands), sodium bicarbonate (Church & Dwight Co., Princeton, NJ), baking powder (ADM Arkady, Olathe, KS), cinnamon and vanilla (Spiceco, Avenel, NJ), xanthan gum and locust bean gum (TIC gums), pregelatinized starch (Instant Pure-Flo), modified flour (Homecraft Create 765, National Starch, Bridgewater, NJ), α-amylases (Grindamyl, Danisco Foods, Brabrand, Denmark), emulsifier blends (Grindsted GA 1350 K-A, blend of propylene glycol ester of fatty acids, monodiglycerides, and sodium stearoyl lactate from Danisco Foods), polydextrose (Danisco Foods), glycerol (Brenntag Southwest Inc., Longview, TX), and polysorbate 60 (Protasorb S20, Protameen Chemicals, Totowa, NJ) were used as ingredients of various cake formulations.

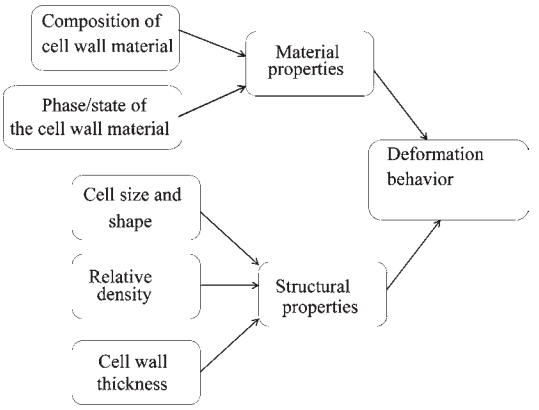

Figure 2. Interrelationship between material−structural−mechanical properties.

Table 1. Chocolate Cake Formulations in Total Weight Percentage

ingredient	cake A (control)	cake B	cake C
water	30.00	29.76	29.84
sugar, extra fine	27.00	26.00	25.28
cake flour	16.00	15.87	15.91
pregelatinized flour	0	1.51	0.76
shortening	11.71	11.22	11.36
glycerol	3.23	3.17	3.18
cocoa	5.00	4.98	4.99
whole eggs, dried	3.80	3.78	3.79
baking powder	0.75	0.75	0.76
salt	0.75	0.72	0.73
instant starch	1.00	0.99	1.00
vanilla	0.09	0.09	0.09
sodium bicarbonate	0.09	0.15	0.15
cinnamon	0.28	0.28	0.28
antimicrobial agent	0.10	0.09	0.10
polysorbate 60	0	0.45	0.46
enzyme	0	0.01	0.01
polydextrose	0	0	0.38
emulsifier	0	0	0.76
guar gum	0.10	0.09	0.10
xanthan gum	0.10	0.09	0.10

Preparation of Cake Samples. In a preliminary study eight different formulations were tested to understand the effect of enzymes, pregelatinized modified flour, polysorbate, gums, polydextrose, and emulsifiers individually on staling (unpublished results). For this purpose we performed accelerated shelf-life testing, and texture was our main quality control parameter. After careful evaluation of the data, we chose the best formulations and combined the ingredients at various levels to obtain recipes B and C.

Three different chocolate cake formulations were baked. Table 1 summarizes the percentages of ingredients used in each formulation. Sample A was control, sample B was a formulation that contained modified flour (1.51%), α-amylase enzyme (0.01%), and gums (0.18%), whereas sample C contained modified flour (0.76%), polydextrose (0.38%), emulsifier (0.76%), α-amylase enzyme (0.01%), and gums (0.20%) different from the basic control formulation.

The mixing and baking protocol of the cakes is summarized in Figure 3. The ingredients were mixed using a Hobart mixer (Hobart Corp.,

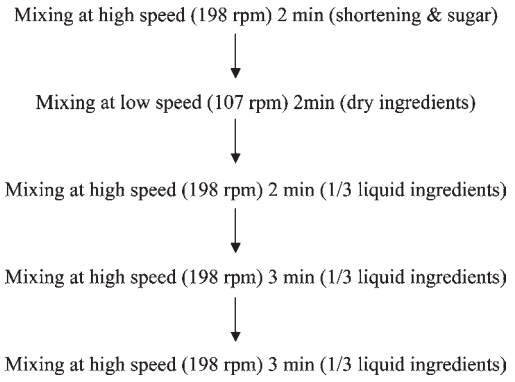

Figure 3. Flow diagram for mixing of ingredients.

Troy, OH) with a batch size of 10 kg. The shortening and sugar were mixed first for 2 min at 198 rpm. The next step in mixing involved the addition of the remaining dry ingredients (flour, baking powder, baking soda, cocoa, dried egg powder, gums, antimicrobial agents, cinnamon, and starch) and mixing the original mixture with them for an additional 2 min at 107 rpm. Next, the liquid ingredients (glycerol, water, and vanilla) were added gradually to the previously mixed dry ingredients and mixed for 2 min at 198 rpm to avoid formation of clumps in the batter and to get homogeneous distribution. This was followed by two more rounds of mixing during which one-third of the remaining liquid ingredients was sequentially added. The specific gravities of the cake batters were 0.92 ± 0.01, 0.89 ± 0.01, and 1.04 ± 0.04 g/cm^3 at 25 °C for samples A, B, and C, respectively. Approximately 1000 g of batter was transferred to the baking trays and baked at 177 °C for 50 min in a rotary oven (Reed Oven Co., Kansas City, MO). During baking 11.72 ± 0.05% water of the total weight evaporated.

The cakes were cooled and hermetically sealed in meals ready to eat (MRE) packages with ferrous-based oxygen scavengers, tray material coextruded structure consisting of ethylene vinyl alcohol and lid material consisting of several layers of polyolefin, aluminum foil, polyamide, and polyester. The samples were grouped in three sets of A, B, and C cake formulations. Cake samples were first stored at 37 and 50 °C for 1 month and then transferred to 4 and 25 °C storage boxes for an additional week.

Microstructural Characterization by X-ray Microtomography and Image Analysis. Cake samples were scanned using the desktop XMT imaging system (model 1072, Skyscan, Aartselaar, Belgium) consisting of an X-ray tube, an X-ray detector, and a CCD camera. The X-ray tube was operated at a voltage/current of 40 kV/250 μA for the cake samples, to obtain optimum contrast of void (air cells) and matter (cell walls). Shadow images were captured using a 12-bit, cooled CCD camera (1024 × 1024 pixels). Samples were scanned at a magnification of 24, resulting in a pixel size of 23.29 μm. Samples were rotated a total of 180° during the scanning process. The exposure time was 1.3 s. X-ray images were obtained every 1.33° of rotation for a total of 137 shadow images (radiographs) per sample. The total scanning time was 15 min.

After scanning, shadow images for each of the samples were loaded into NRecon reconstruction software (V1.5.1.). This software combines the images graphically into a 3-D object from which 2-D cross-sectional images can be taken. Before the reconstruction process, the CS rotation feature was used to rotate the (sample) cross sections, making them parallel to the view window. All substances attenuate low-energy X-ray beams stronger than high-energy X-ray beams due to photoelectric absorption. A heterogeneous X-ray beam passing through an absorbing object becomes more penetrating. This phenomenon is called beam hardening, which might cause different artifacts in the reconstructed image; to reduce artifacts, beam hardening was set at 40%. Reconstructions of the gray scale histograms were set at a dynamic range of 0.015−0.060 for cake samples. The low gray value (low absorption coefficient) within the sample matrix referred to air cells.

Three-dimensional image analysis was carried out with CTan software (release 1.5.0.2; SkyScan), which computed 3-D parameters from the stack of 2-D sections after segmentation. The volume of interest (VOI) was designed by interactively drawing circles on the 2-D gray images before reconstruction. Such circles were drawn only on a few sections (starting, middle, and final sections), and a routine facility calculated all of the intermediary masks by interpolation. The parameters and distributions of cell wall thickness and cell size together with fragmentation index (measure of cell connectedness) were obtained by the CTan software.

Textural Characterization. Cake samples were cut cylindrically (diameter = 5 cm, height = 4 cm) with an in-house designed mold. Texture measurements were performed with a TA.XT2i Texture analyzer (Texture Technologies Corp., Scarsdale, NY), equipped with a 25 kg load cell and a 5 cm aluminum cylindrical probe. Uniaxial compression was applied at a test speed of 1 mm/s and 60% strain level. Data were collected at 200 points per second (pps) and processed using Texture Exceed Expert (TEE) software version 2.61 (Texture Technologies Corp.). Resulting force-deformation curves were used for the evaluation of textural parameters, and the data were reported as the average of 10 replicate measurements. Toughness, which was the energy response of the material against deformation, was calculated from the area under the maximum force value of the force-displacement curve.

X-ray Diffraction Analysis for Determination of Crystallinity. The wide-angle X-ray scattering (WAXS) patterns of cake samples were obtained using a Bruker HiStar area detector and an Enraf-Nonius FR571 rotating anode X-ray generator equipped with a graphite monochromator (Cu Kα; λ = 1.5418 Å) operating at 40 kV and 50 mA. All of the data were collected at room temperature over a period of about 1800 s. The sample to detector distance was 9.0 cm, and the standard spatial calibration was performed at that distance. Scans were 4° wide in omega (ω) with fixed detector, or Bragg, angle (2θ) of 25°, and fixed χ angle of 0 and freely spinning Φ angle. In all cases, the count rate for the area detector did not exceed 100,000 cps. The samples were prepared by forcing the fine cake into the open end of a 1 mm special glass X-ray capillary. The open end of the capillary with sample was forced into a clay mounting on the goniometer head. The center of the capillary was centered on the instrument. The intensity versus 2θ plots were fitted into the SigmaScan Pro software for image analysis according to the method of Cheetham and Tao[20] as shown in Figure 4. A smooth curve that connected the peak baselines was plotted on the diffractograms. The area above the peak baseline corresponded to the crystalline portion, and the lower area between the smooth curve and a linear baseline that connected the initial and final 2θ values was taken as the amorphous region. Percent relative crystallinity was calculated from the following equation:

$$\text{relative crystallinity (\%)} = \frac{\Sigma \text{ area under peaks}}{\text{area of amorphous region}}$$

RESULTS AND DISCUSSION

Cakes fall into the group of soft cellular solid food products in which the morphological parameters can be controlled by the type of ingredients, formulation, and baking conditions. A good-quality cake should have high volume with a fine uniform moist crumb. Cake batters go through a series of processes during which they transform from wet foam to dry foam. The protein phase (especially egg proteins) forms a network around air bubbles to stabilize them. Wet protein foam consisting of egg proteins, fat, and emulsifiers is blended with dry ingredients of sugar, flour, and cocoa. This step is the most important mixing

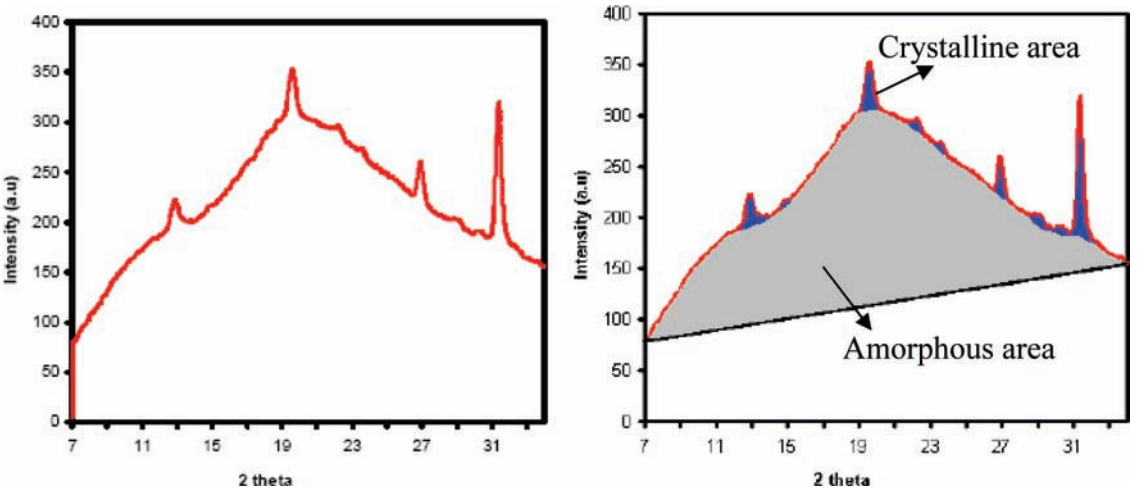

Figure 4. Relative crystallinity calculations for cakes by the use of SigmaScan Pro image analysis software (according to the method from ref 20).

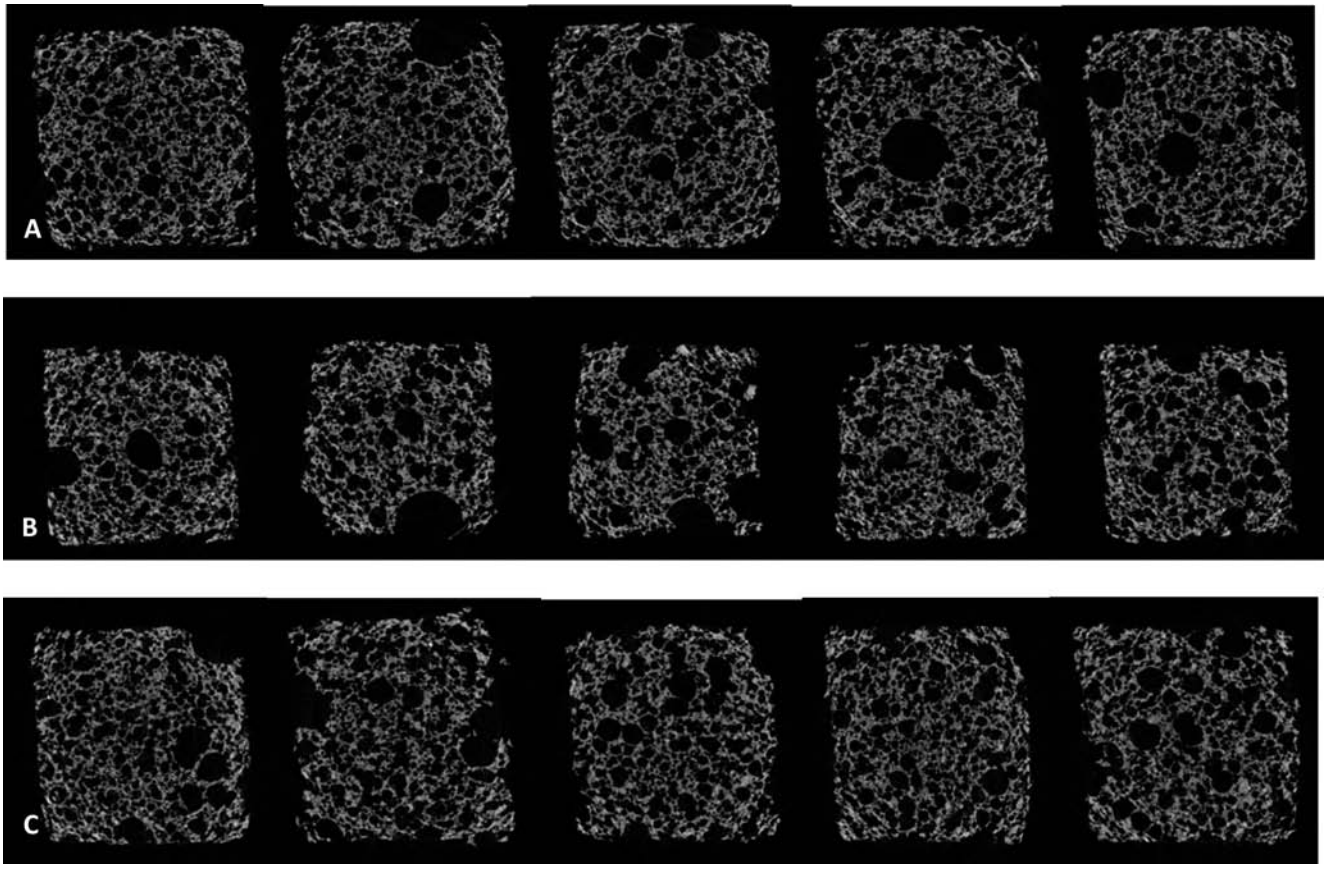

Figure 5. XMT 2-D reconstructed cross-section images of cake samples A−C.

step, during which small molecules (sugar) and polymers (flour, cocoa) are incorporated into the formulation.[21] The cake formulations used in this study contained high levels of sucrose, which are claimed to increase foam stability in the literature.[22] Sugar as an ingredient also has the ability to increase starch gelatinization and protein denaturation temperatures, which was stated to improve air bubble expansion during baking.[23−27] During baking some of the preformed bubbles fail due to surrounding film rupture. However, the starch gelatinization, together with protein denaturation, holds the structure together and maintains air pockets. The higher the number of air pockets inside the cake, the more porous the structure becomes and the higher the final product volume.[28]

From a materials science approach solid cellular materials can be categorized on the basis of the shape of the cells as being open or closed cell foams. Open cell structured porous food materials consist of pores that are connected to each other through an interconnected network, which is relatively soft compared to

closed cell foam structures. The closed cell foams do not have interconnected pores, and they have higher compressive strength due to their dense structures. Figure 5 represents the 2-D cross-sectional images obtained with X-ray microtomography from the data set of the reconstructed images. Cake samples were taken from the center of each tray and put into transparent zip-lock bags to avoid moisture loss prior to and during analysis with X-ray microtomography. The images show the air pockets within the solid protein, carbohydrate, and fat network. According to these images cake samples had mostly open cell structure with embedded closed cells located at the sides and near the crust of the cake sample. Due to their less dense structure open cell foams show a tendency to fill with the fluid that surrounds it. In the cake samples this phenomenon results in free relocation of water throughout the cake crumb from sites that have more water (e.g., center) to less water-concentrated sites (e.g., crust and edges).[29] We hypothesize that moisture redistribution throughout the porous structure relocates the water that is contributing to starch retrogradation during storage. Hardening of the cake crumb is also related to moisture redistribution from inside to outside. Thus, controlling the moisture migration from inside to outside crumb can slow the starch retrogradation rate.

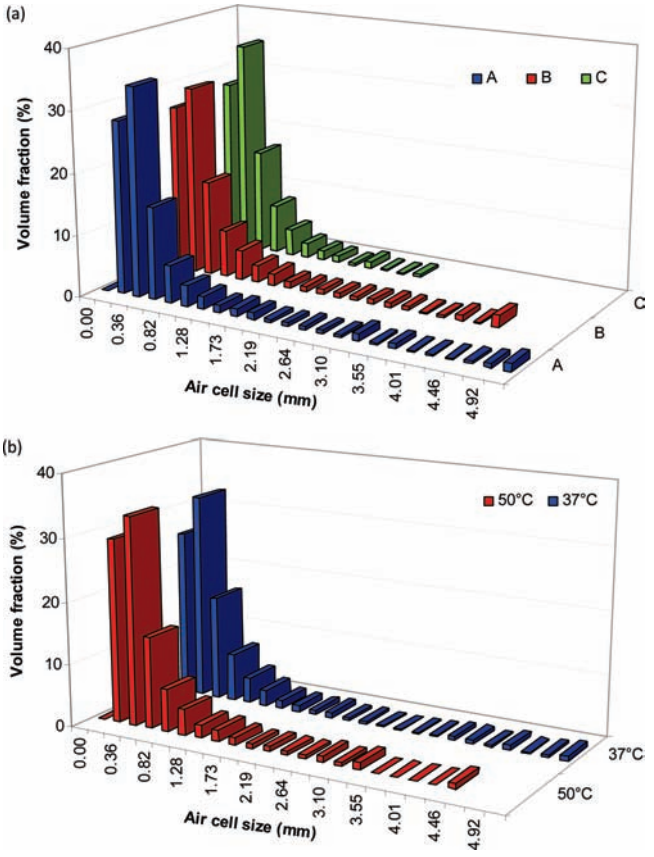

Figure 6. Air cell size distributions with respect to (a) formulation and (b) storage temperature.

Cake volume is related to the amount of air incorporated in the baked product. However, cakes with similar volumes can be quite different in bubble size distribution. Yang et al.[30] found that with increasing sugar concentration in cakes, where foam structure is assured by egg white protein, the air bubbles became finer as the cake height became higher. These two phenomena are indicators of a stable foam structure. Yang and Foegeding[31] found that large bubbles in cake structure indicated disproportionation and coalescence, which occurred before the foam settled to a cellular solid structure during baking. The same authors also reported that egg white protein cakes together with high sugar levels prevented bubble disproportionation and yielded finer structure cake.

The X-ray tomography technique has been used by many to evaluate cellular morphology based on reconstructed 2-D slice images and the rendered 3-D model.[16,17,32−35] In cellular solid food systems the 2-D image analysis does not consider structural variations from one slice to another. In fact, arbitrary 2-D images are taken from a stack of images, whereas in 3-D image analysis the complete set is used for analysis. The bubble formation process during baking can involve specific information mainly in the third orthogonal dimension. To represent the data from orthogonal dimension, we performed 3-D analysis. The 3-D porous structure was lowest for sample B and highest for sample A in all storage conditions (Figure 6).

Analysis of 3-D XMT images of cake samples showed that the cellular structure of cake samples A−C varied with average cell area of 0.130−0.630 mm^2 and t/R ratio of 0.137−0.489 (Tables 2 and 3). Generally, all of the cake samples consisted of several small pores, which have pore areas ranging between 0.13 and 1.80 mm^2 and between 0.18 and 0.63 mm^2 for samples stored at 37 and 50 °C, respectively. The control sample (cake A) was found to have the widest range of air cell distribution followed by cakes B and C regardless of storage temperature (Figure 6a). Storage temperature had a less pronounced effect on the cell size distribution compared to that of cake formulation (Figure 6b). Cake C had relatively thicker cell walls (Figure 7a),

Table 2. Parameters of Image Analysis for Cake Samples Kept at 37 °C

storage conditions	cake type	av cell area (A, mm^2)	av cell radius (R, mm)	av cell wall thickness (t, mm)	t/R
37 °C (1 month)	A	1.800	1.344	0.184	0.137
	B	0.670	0.821	0.195	0.237
	C	0.380	0.617	0.188	0.305
37 °C (1 month) + 4 °C (1 week)	A	0.130	0.366	0.179	0.489
	B	0.620	0.788	0.193	0.244
	C	0.210	0.458	0.187	0.409
37 °C (1 month) + 25 °C (1 week)	A	0.360	0.600	0.177	0.296
	B	0.340	0.576	0.187	0.326
	C	0.260	0.504	0.192	0.380

Table 3. Parameters of Image Analysis for Cake Samples Kept at 50 °C

storage conditions	cake type	av cell area (A, mm^2)	av cell radius (R, mm)	av cell wall thickness (t, mm)	t/R
50 °C (1 month)	A	0.630	0.793	0.176	0.222
	B	0.470	0.687	0.181	0.264
	C	0.290	0.540	0.173	0.321
50 °C (1 month) + 4 °C (1 week)	A	0.220	0.469	0.175	0.374
	B	0.620	0.788	0.193	0.244
	C	0.180	0.427	0.180	0.420
50 °C (1 month) + 25 °C (1 week)	A	0.564	0.751	0.175	0.233
	B	0.410	0.643	0.198	0.308
	C	0.251	0.501	0.168	0.335

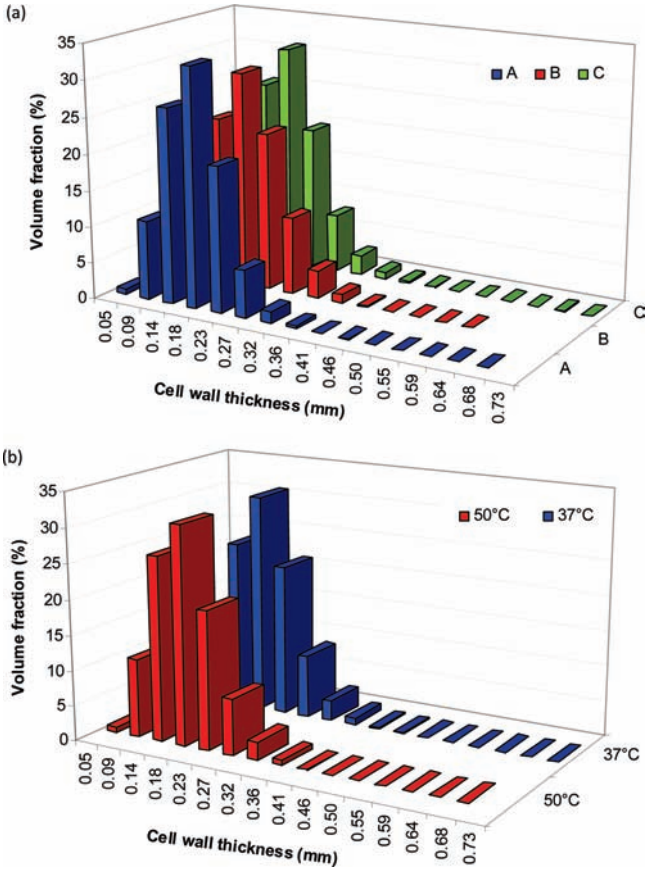

Figure 7. Cell wall thickness distributions with respect to (a) formulation and (b) storage temperature.

leading to a significantly higher thickness to radius ratio (0.367) than the ratios observed for cakes A (0.303) and B (0.271). Similar to cell size distributions, storage temperature had a less pronounced effect on cell wall thickness distributions (Figure 7b) than did cake formulation. Cake C batter was thicker than the other samples. Unlike the other formulations, it contained gum−polydextrose and emulsifier combinations. Cake C had limited expansion rate of bubbles, resulting in smaller air cells with thicker cell walls. The use of emulsifiers in the formulation narrowed the size difference within air cells. A slight decrease of cell wall thickness was observed for cake samples stored at 50 °C together with a decrease in cell diameter (Figures 6 and 7). The decrease in cell diameter was more pronounced than the decrease in cell wall thickness, resulting in a high t/R ratio.

Macroscopic deformation behavior of porous food samples can be predicted from their cell structure. The total energy of the cakes falls within the group of ductile foams, where the strain energy remains convex for the entire range of the applied displacements. Figure 8 represents the mechanical response of cake samples under uniaxial compression. In the first region all of the samples exhibited a linear portion that was accompanied by a stress plateau represented as region 2 in Figure 8. The stress plateau is associated with the buckling of the solid network surrounding the air cells.[36] Toughness and thickness to radius ratio of cakes showed a positive correlation with regression values of 0.68 and 0.95 for the samples stored and cycled at 37 and 50 °C, respectively (Figures 9 and 10). As the foams became less dense, with thickness to radius ratio approaching zero (larger air cells with thinner cell walls), the textural parameters of hardness and toughness were expected to decrease. In samples B and C, where the porous structure was controlled by using emulsifiers and surfactants, sample B had the lowest t/R ratio at 37 °C storage conditions, resulting in lower toughness values. The diversity in cell size distribution of sample A made it difficult to find a general trend between the structural and textural parameters. The effect of storage conditions on structural parameters was higher for cake samples stored at 50 °C. Both toughness and t/R ratio for cake samples stored at 50 °C were higher than for the cake samples stored at 37 °C (Figure 9). As the diameter of the cells/pores decreased, the resistance to the applied forces increased. Even though the samples were stored in sealed packages, water was released from the cake samples stored at high temperatures to the headspace. During storage of cakes, water has been reported to transfer from the soft and wet core to the outside drier crust.[29]

The toughness of samples stored at 37 °C was less structure dependent and showed relatively less change in toughness in the range of 55−61 N·s. The change in texture was not associated with the structural t/R ratio, and they exhibited less crystallinity with a pronounced rubbery state (Table 4). It is reported in the literature that as staling proceeds, water becomes more bound and immobilized.[37] However, at a high storage temperature of 50 °C, cake toughness is strongly influenced by the structural parameters. A high t/R ratio caused the toughness values to increase significantly up to 90 N·s. The increase in percent relative crystallinity of the cake samples at high temperatures, notably, to low-temperature cycles made cakes harder and more structure-dependent. Under all storage conditions, the control

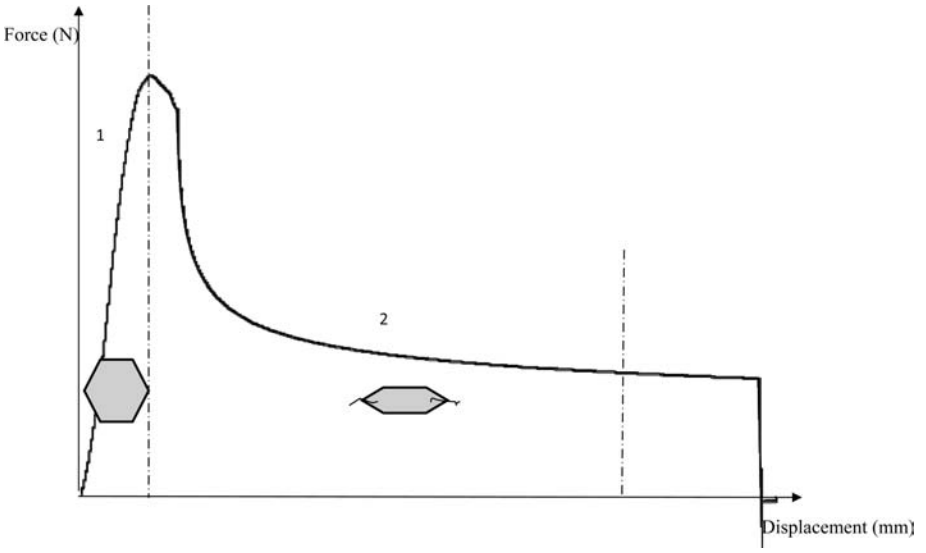

Figure 8. Effect of structure on force displacement curve.

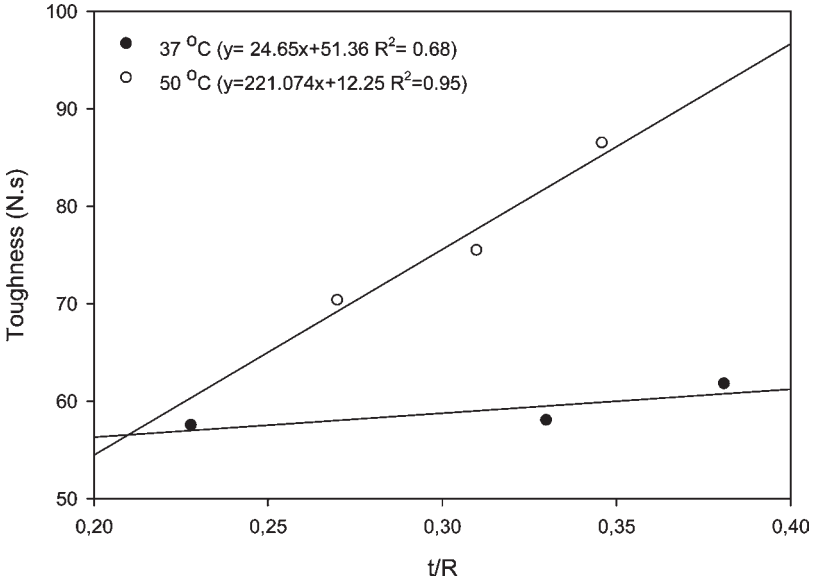

Figure 9. Effect of t/R ratio on cake toughness (analysis results of 3-D analysis).

cake (sample A) had higher crystallinity because there was less control over moisture redistribution as compared to samples B and C. Starch crystallization was also found to influence the firmness and toughness in cake samples relative to storage conditions (Figure 10). If the starch recrystallization rates of cakes were compared on the basis of the differences in ingredients, cake sample C gave the lowest percentage of relative crystallinity. The polydextrose in the cake C formulation acts as both a bulking agent and a texturizer. On the other hand, the emulsifiers form a complex with amylase, interfering with the starch recrystallization. The pregelatinized flour, which is used in a higher amount in cake sample B, rehydrates easily and contributes to the viscosity of the batter, reducing the moisture loss during baking and storage. Chemical modifications control the rate of rehydration of a pregelatinized starch. The higher the degree of stabilization, the slower the hydration rate and the less it contributes to batter viscosity.[38]

The thickness to radius ratio (t/R) can also be associated with the total energy of the thin-walled air cells. The total energy of a porous material subjected to uniaxial stress is the sum of the in-plane stretch deformation $(W_s(F))$ and the bending deformation $(W_b(F))$, which is given by the following equation:[39]

$$W(F) = W_s(F) + W_b(F) = \frac{1}{2}E(R^2 t W_1(F)) + \frac{1}{12}t^3 W_2(F) \quad (2)$$

To estimate the strain−energy density, a representative volume (V_0) needs to be calculated where the air cells are assumed to be spherical with a volume of $(4/3)\pi R^3$. The strain energy density (W) will be

$$W = \frac{W}{V_0} = \frac{3}{8\pi}E\left[\frac{t}{R}W_1(F) + \frac{1}{12}\left(\frac{t}{R}\right)^3 W_2(F)\right] \quad (3)$$

dx.doi.org/10.1021/jf103766x |J. Agric. Food Chem. 2011, 59, 1498–1507

From the equation above, the contribution from in-plane stretch is a linear function of the t/R ratio, whereas the bending is a function of $(t/R)^3$. Also, because relative density is the fraction of the solid contained in the representative volume, equal to $\rho = 3(t/R)$, the stretch contribution scales linearly with ρ and the bending with its cubic power.[39] The mathematical relationship we identified between the toughness and thickness to radius ratio (t/R) is in agreement with the third-order nonlinear relationship between t/R and strain−energy density provided by Cuitino et al.[39] Experimentally, it was observed that cake samples with dense structures consisting of small air cells with thick cell walls gave higher energy response to deformation.

Relative density, which is mentioned above, has been shown to be the dominant physical characteristic representing the 3-D structure of cellular solids. Various authors used the relative density approach to understand the solid mechanics of food products.[40−45] However, the relative density is not a standalone tool to be used to evaluate the mechanical properties of fracture, because solid foams with identical relative densities might yield different mechanical responses to deformation.[18] Cell structure, the beams and cell walls that form the solid phase of cellular solid foods, density, and overall morphological characteristics should be considered as a whole concept to explain the textural properties of cellular solid foods.

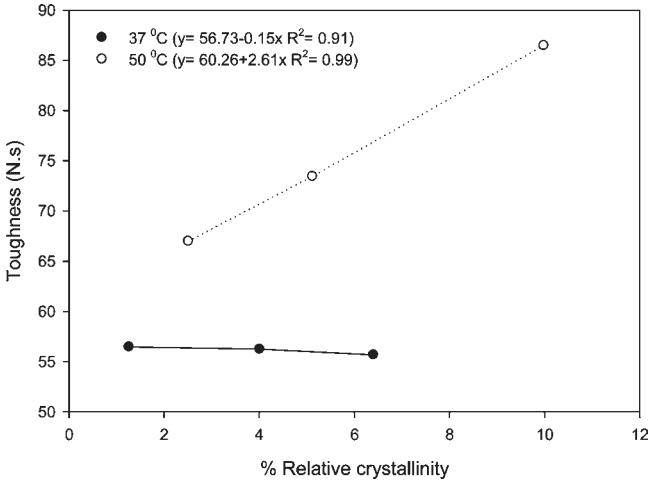

Figure 10. Effect of percent relative crystallinity on cake toughness.

The fragmentation index (FI) is a measure of the relative connectivity of the cell wall structure. FI measures the relative convexity or concavity of the total surface, which is calculated on the principle that concavity indicates connectivity (and the presence of nodes) and convexity indicates isolated disconnected structures (struts). Fragmentation indices of cake samples, obtained by 3-D image analysis, are shown in Figure 11. A lower fragmentation index (i.e., higher negative values) signifies better connected lattices, whereas a higher value of FI indicates more

Table 4. Percent Relative Crystallinity of Samples Stored at 37 and 50 °C

sample	37 °C (1 month)	37 °C (1 month) + 25 °C (1 week)	37 °C (1 month) + 4 °C (1 week)
A	2.32	5.70	8.09
B	0.95	4.62	6.42
C	0.51	1.70	4.70
sample	50 °C (1 month)	50 °C (1 month) + 25 °C (1 week)	50 °C (1 month) + 4 °C (1 week)
A	4.23	7.23	10.73
B	2.20	5.37	9.73
C	1.10	2.78	9.50

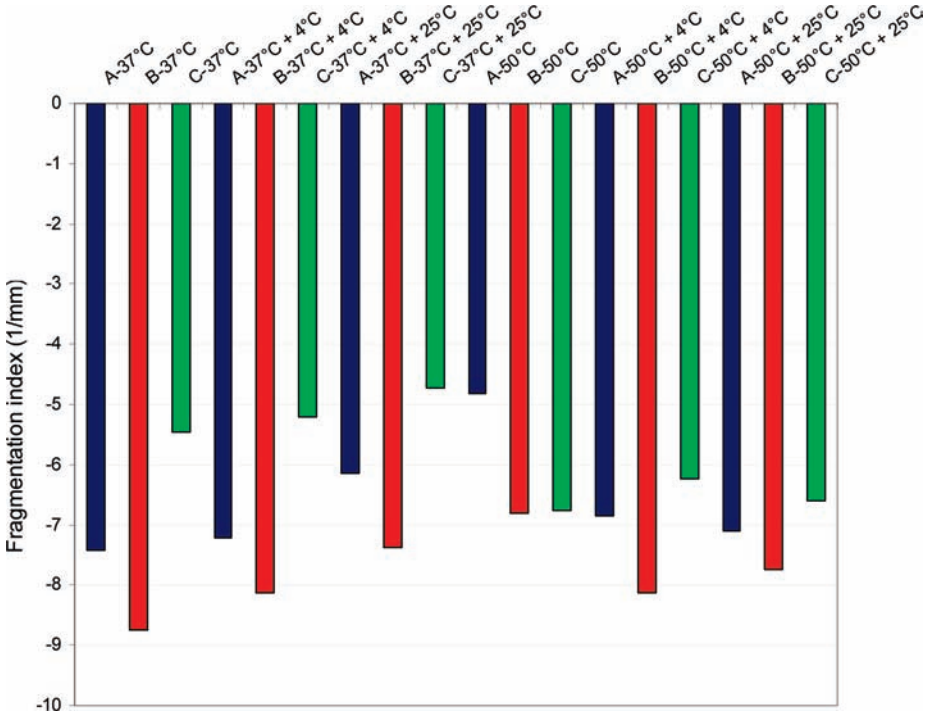

Figure 11. Fragmentation index (degree of cell connectedness) for cake samples.

dx.doi.org/10.1021/jf103766x |J. Agric. Food Chem. 2011, 59, 1498–1507

disconnected void (air cell) structures.[46] In all cases of various storage conditions fragmentation indices ranged between −4.7 and −8.8, indicating high connectivity of the pores (i.e., open cell structure). However, when we looked closely at the values for the three different formulations, the fragmentation index value was relatively higher for cake C. Cake C had more connectivity within the closed structure with lowest average cell size based on 3-D analysis results with respect to cake formulation. This resulted in the highest t/R ratio accompanied with high toughness values for these samples.

In conclusion, this study has shown the use of a combined X-ray microtomography technique and three-dimensional image analyses to illustrate the effect of microstructural properties on cake samples, which belong to the group of soft cellular solid food materials. A high correlation between the structural parameter, the thickness-to-radius ratio, and textural toughness was found. The air cell size and air cell size distributions together with the fragmentation index values provided detailed information on the porous structure of the cake samples. Three-dimensional image analyses of high-quality processed images can also be used in the food industry as a reliable and accurate control of heterogeneous food structure, which can be further used to understand the relationship between texture−sensory properties of cellular solid foods and food morphology.

AUTHOR INFORMATION

Corresponding Author

*E-mail: kokini@illinois.edu.

Funding Sources

This project was supported by the U.S. Department of Defense, under Contract SP0103-02-D-0024, Delivery order 0016, Title: STP#2027: Quality Improvement Project for Shelf Stable Bakery Products and National Research Initiative of the USDA Cooperative State Research, Education and Extension Service, Grant 2006-35503-18969.

REFERENCES

(1) Dogan, H.; Kokini, J. L. Psychophysical markers for crispiness and influence of phase behavior and structure. *J. Texture Stud.* **2007**, *38*, 324–354.

(2) Barrett, A. H.; Peleg, M. Extrudate cell structure−texture relationships. *J. Food Sci.* **1992**, *57*, 1253–1257.

(3) Scanlon, M. G.; Zghal, M. C. Bread properties and crumb structure. *Food Res. Int.* **2001**, *34*, 841–864.

(4) Barrett, A. H.; Cardello, A. V.; Lesher, L. L.; Taub, I. A. Cellularity, mechanical failure, and textural perception of corn meal extrudates. *J. Texture Stud.* **1994**, *25*, 77–95.

(5) Kalab, M.; Allan-Wojtas, P.; Miller, S. S. Microscopy and other imaging techniques in food structure analysis. *Trends Food Sci. Technol.* **1995**, *6*, 177–186.

(6) Ferrando, M.; Spiess, W. E. L. Review: Confocal scanning laser microscopy. A powerful tool in food science. *Food Sci. Technol. Int.* **2000**, *6* (4), 267–284.

(7) Maas, J. L.; Line, M. J. Nuclear magnetic resonance microimaging of strawberry flower buds and fruit. *Hortic. Sci.* **1995**, *30*, 1090–1096.

(8) Ramos-Cabrer, P.; Duynhoven, J. P. M.; van Dalen, G.; Nicolay, K. MRI: assessment of water transport in food. *Cienc. Frontera* **2005**, *3* (1), 59–66.

(9) Hullberg, A.; Ballerini, L. Pore formation in cured-smoked pork determined with image analysis − effects of tumbling and RN- gene. *Meat Sci.* **2003**, *65* (4), 1231–1236.

(10) Du, C.-J.; Sun, D.-W. Automatic measurement of pores and porosity in pork ham and their correlations with processing time, water content and texture. *Meat Sci.* **2006**, *72* (2), 294–302.

(11) Rahman, M. S.; Al-Amri, O. S.; Al-Bulushi, I. M. Pores and physico-chemical characteristics of dried tuna produced by different methods of drying. *J. Food Eng.* **2002**, *53* (4), 301–313.

(12) Kassama, L. S.; Ngadi, M. O. Pore structure characterization of deep-fat-fried chicken meat. *J. Food Eng.* **2005**, *66* (3), 369–375.

(13) Falcone, P. M.; Baiano, A.; Zanini, F.; Mancini, L.; Tromba, G.; Montanari, F.; Nobile, M. A. A novel approach to the study of bread porous structure: phase-contrast X-ray microtomography. *J. Food Sci.* **2004**, *69* (1), FEP38–FEP43.

(14) Trater, A. M.; Alavi, S.; Rizvi, S. S. H. Use of non-invasive X-ray microtomography for characterizing microstructure of extruded biopolymer foams. *Food Res. Int.* **2005**, *38* (6), 709–719.

(15) Leonard, A.; Blacher, S.; Nimmol, C.; Devahastin, S. Effect of far-infrared radiation assisted drying on microstructure of banana slices: an illustrative use of X-ray microtomography in microstructural evaluation of a food product. *J. Food Eng.* **2008**, *85* (1), 154–162.

(16) Lassoued, N.; Babin, P.; Della Valle, G.; Devaux, M. F.; Réguerre, A. L. Granulometry of bread crumb grain: contributions of 2-D and 3-D image analysis at different scale. *Food Res. Int.* **2007**, *40*, 1087–1097.

(17) Maire, E.; Fazekas, A.; Salvo, L.; Dendievel, R.; Youssef, S.; Cloetens, P.; Letang, J. M. X-ray tomography applied to the characterization of cellular materials. Related finite element modeling problems. *Compos. Sci. Technol.* **2003**, *2431*, 2443.

(18) Dogan, H.; Romero, P. A.; Zheng, S.; Cuitino, A. M.; Kokini, J. L. Characterization and prediction of the fracture response of solid food foams. In *Bubbles in Foods 2: Novelty, Healthy, Luxury International Conference Proceeding Book*; Campbell, G. M., Scanlon, M. C., Pyle, D. C., Eds.; American Association of Cereal Chemists: St. Paul, MN, 2007; pp

(19) Szczesniak, A. S. Texture is a sensory property. *Food Qual. Pref.* **2002**, *13*, 215–225.

(20) Cheetham, N. W. H.; Tao, L. Variation in crystalline type with amylose content in maize starch granules: an X-ray powder diffraction study. *Carbohydr. Polym.* **1998**, *36*, 277–284.

(21) Berry, T. K.; Yang, X.; Foegeding, A. E. Foam prepared from whey protein isolate and egg white protein: 1. Changes associated with angel food cake functionality. *J. Food Sci.* **2009**, *74*, E269–E277.

(22) Ochi, A.; Katsuta, K.; Maruyama, E.; Kubo, M.; Ueda, T. Effects of sugars on stability of egg foam and their rheological properties. In *Hydrocolloids* − Part 2; Nishinari, K., Ed.; Elsevier Science: Amsterdam, The Netherlands, 2000; pp 275.

(23) Munzing, K.; Brack, G. DSC-studies of flour confectionery. *Thermo. Acta.* **1991**, *187*, 167–173.

(24) Ngo, W. H.; Taranto, M. V. Effect of sucrose level on the rheological properties of cake batters. *Cereal Foods World* **1986**, *31* (4), 317–322.

(25) Pernell, C. W.; Luck, P. J.; Foegeding, A. E.; Daubert, C. R. Heat-induced changes in angel food cakes containing egg-white protein or whey protein isolate. *J. Food Sci.* **2002**, *67* (8), 2945–2951.

(26) Kim, S. S.; Setser, C. S. Wheat starch gelatinization in the presence of polydextrose or hydrolyzed barley β-glucan. *Cereal Chem.* **1992**, *69*, 447–452.

(27) Kim, S. S.; Walker, C. E. Effects of sugars and emulsifiers on starch gelatinization evaluated by differential scanning calorimetry. *Cereal Chem.* **1992**, *69* (2), 212–217.

(28) Handleman, A. R.; Conn, J. F.; Lyons, J. W. Bubble mechanics in thick foams and their affects on cake quality. *Cereal Chem.* **1961**, *38*, 294.

(29) Guy, R. C. E. Factors affecting the staling of Madeira slab cake. *J. Sci. Food Agric.* **1983**, *34*, 477–491.

(30) Yang, X.; Berry, T. K.; Foegeding, A. E. Foams prepared from whey protein isolate and egg white protein: 1. Physical, microstructural, and interfacial properties. *J. Food Sci.* **2009**, *74*, E259–E268.

(31) Yang, X.; Foegeding, A. E. Effects of sucrose on egg white protein and whey protein isolate foams: factors determining properties of wet and dry foams (cakes). *Food Hydrocolloids* **2010**, *24* (227), 238.

(32) Bikard, J.; Coupez, T.; Della Valle, G.; Vergnes, B. Simulation of bread making process using a direct 3D numerical method at microscale: analysis of foaming phase during proofing. *J Food Eng.* **2008**, *85*, 259–267.

(33) Brydon, A. D.; Bardenhagen, S. G.; Miller, E. A.; Seidler, G. T. Simulation of the densification of real open-celled foam structures. *J. Mechanics Physics Solids* **2005**, *53*, 2638–2660.

(34) Lim, K. S.; Barigou, M. X-ray micro-computed tomography of cellular food products. *Food Res. Int.* **2004**, *37* (10), 1001–1012.

(35) Babin, P.; Della Valle, G.; Dendievel, R.; Lourdin, D.; Salvo, L. X-ray tomography study of the cellular structure of extruded starches and its relations with expansion phenomenon and foam mechanical properties. *Carbohydr. Polym.* **2007**, *68* (2), 329–340.

(36) Gioia, G.; Wang, Y.; Cuitino, A. M. The energetic of heterogeneous deformation in open cell solid foams. *Proc. R. Soc. London A* **2001**, *457*, 1079–1096.

(37) Grenier, D.; Le Ray, D.; Lucas, T. Combining local pressure and temperature measurements during bread baking: insights into crust properties and alveolar structure of crumb. *J. Cereal Sci.* **2010**, *52*, 1–8.

(38) Oreopoulou, V. Fat replacers. In *Fat Replacers in Bakery Products*; Yiu, H., Corke, H., Nip, W., De Leyn, I., Eds.; Blackwell Publishing: Ames, IA, 2006; pp 193−210.

(39) Cuitino, A. M.; Zheng, S. Taylor averaging on heterogeneous foams. *J. Compos. Mater.* **2003**, *37*, 701–713.

(40) Keetels, C. J. A. M.; Van Vliet, T.; Walstra, P. Relationship between the sponge structure of starch bread and its mechanical properties. *J. Cereal Sci.* **1996**, *24*, 27–31.

(41) Keetels, C. J. A. M.; Visser, K. A.; Van Vliet, T.; Jurgens, A.; Walstra, P. Structure and mechanics of starch bread. *J. Cereal Sci.* **1996**, *24*, 15–26.

(42) Zghal, M. C.; Scanlon, M. G.; Sapirstein, H. D. Cellular structure of bread crumb and its influence on mechanical properties. *J. Cereal Sci.* **2002**, *36*, 167–176.

(43) Gibson, L. J.; Ashby, M. F. *Cellular Solids: Structure and Properties*; Cambridge University Press: Cambridge, U.K., 1997.

(44) Warburton, S. C.; Donald, A. M.; Smith, A. C. The deformation of brittle starch foams. *J. Mater. Sci.* **1990**, *25*, 4001–4007.

(45) Lourdin, D.; Della Valle, G.; Colonna, P. Influence of amylose content on starch films and foams. *Carbohydr. Polym.* **1995**, *27*, 261–270.

(46) Hahn, M.; Vogel, M.; Pompesius-Kempa, M.; Delling, G. Trabecular bone pattern factor − a new parameter for simple quantification of bone microarchitecture. *Bone* **1992**, *13* (4), 327–330.